Circuit-equivalent Models for Current-controlled Inverters

Brian Johnson*, Minghui Lu*, Victor Purba†, and Sairaj Dhople†
*Department of Electrical and Computer Engineering, University of Washington, Seattle, WA 98195
†Department of Electrical and Computer Engineering, University of Minnesota, Minneapolis, MN 55455
Emails: {brianbj, mhlu}@uw.edu, and {purba002, sdhople}@umn.edu

***Abstract*—In this paper, we introduce a method to analyze three-phase inverters with current control as equivalent circuits. In contrast to existing methods, both the averaged power stage model *and* its closed-loop controller are represented as a single unified circuit. Since the complete system can be examined as *one* equivalent circuit, we can glean several insights on design and operation; particularly relating to the time scales at which the controller tracks reference signals and the ability to reject disturbances. We leverage the insights afforded by this general approach to outline design strategies for controllers in both synchronous and stationary reference frames.**

I. Introduction

Three-phase dc-ac inverters are ubiquitous across a variety of energy-conversion and grid applications. State-of-the-art approaches for modeling dc-ac inverters are mainly focused on averaged power-stage models and their linearized representations for small-signal analysis [1]. In this paper, we propose a novel framework to model and analyze the control- and averaged physical-layer dynamics of inverters as a single equivalent circuit. In essence, we show that well-known control strategies can be equivalently understood as instances of circuit laws. This allows us to recast the closed-loop system as an equivalent circuit composed of elementary components (e.g., individual passive RLC elements, current sources, voltage sources) and apply a circuit-driven approach to control design. The proposed approach is intuitive, and it yields several insights that facilitate controller design. We also anticipate the unified circuit-based description would facilitate analysis (e.g., stability analysis of networks of inverters).

Related to our approach are impedance-based modeling methods. Under such frameworks, the inverter output terminal is modeled as an ideal source in conjunction with an equivalent impedance whose characteristics are based on the linearized control loops [2]–[5]. Although this method is related to circuit analysis, models in this setting do not represent the control loops explicitly as circuits. Hence, a circuit model with elementary constituent components is not realized. Also related to this work are analog control methods for inverters [6]. While these controllers are implemented with op-amp circuits, our approach is principally different since it is geared towards modeling and accounts for the representation of the full closed-loop system. Finally, we bring to attention control strategies that involve inverters emulating dynamics of nonlinear oscillator circuits [7] and synchronous machines [8] that innately yield equivalent-circuit representations.

For the case of current-controlled three-phase inverters, we demonstrate how algebraic relationships inherent in feedback loops and feedforward paths are translated to equivalent-circuits via elementary circuit laws. Our work differs from some of the related methods referenced above in the sense that the component-level structure of the equivalent circuit is laid bare and its realization does not require linearization. This modeling formalism is useful since it eliminates the boundary that has hitherto separated control- and physical-layer dynamics. Hence, the relationships between the various control signals and physical variables are clearly illustrated and this allow one to apply circuit-inspired rules of thumb to design. Along these lines, we first show how proportional-integral (PI) and proportional-resonant (PR) compensators, as commonly seen in the synchronous dq and stationary $\alpha\beta$ frames, respectively, take the form of RLC circuits. Once this is established, it becomes apparent that the tuning of such controllers is tantamount to a circuit design problem where the time constants of the various circuits are to be systematically determined based on the desired closed-loop performance. This is in contrast to established approaches in the dq [1], [9], [10] and $\alpha\beta$ [11]–[13] frames where design is transfer-function-based and physical intuition is lost. In summary, our paper provides the following contributions: i) we show that current-control feedback and feedforward loops intrinsically embed Kirchhoff's Laws within them and leverage this foundational tenet to formulate a unified circuit model for three-phase inverters, ii) within the context of current control for inverters, we define a one-to-one consistency between circuit laws and classical control laws, and iii) we propose a circuit-driven design methodology for inverters in both the dq and $\alpha\beta$ frames building on circuit-theoretic principles.

The remainder of this paper is organized as follows. Circuit-equivalent modeling basics are introduced in Section II. Models for the synchronous dq and the stationary $\alpha\beta$ frame are provided in Section III. Numerical simulation results are provided in Section V. Concluding remarks are in Section V.

Funding was provided in part by the U.S. Department of Energy Office of Energy Efficiency and Renewable Energy Solar Energy Technologies Office grant number DE-EE0008346, and the National Science Foundation through grant ECCS-1453921.

978-1-7281-1842-0/19/$31.00 ©2019 IEEE

II. Circuit Modeling Primer

To familiarize the reader with the circuit-equivalent model concept, we begin with the half bridge converter with current control in Fig. 1(a). An output filter with inductance L and parasitic resistance R interfaces the converter output with the network. The voltage v_o generically represents the voltage across any active load, passive load, stiff voltage source, or any combination thereof. The output current, i, is measured and compared to the reference $i^\star$. The error, $e := i^\star - i$, is fed to a compensator, G_c, which produces the control effort u. Subsequently, the output voltage, v_o, is used as a feedforward signal which is added to u to produce the terminal voltage command $v_\mathrm{t}^\star$. Lastly, the terminal command is scaled by the dc-side input voltage, v_dc, and processed by pulse width modulation (PWM) such that the converter terminal voltage, v_t, tracks $v_\mathrm{t}^\star$.

From here forward, we consider switch-cycle-averaged quantities such that PWM is abstracted away and $v_\mathrm{t} = v_\mathrm{t}^\star$. Reflecting on the well-known structure in Fig. 1(a), it is evident that the compensator translates current differences into a voltage signal u. Hence, the input and output sides of the control block-diagram can be construed as instances of Kirchhoff's current and voltage laws, respectively. Since G_c translates a current signal into a voltage signal, it follows that the compensator itself is an impedance which we denote interchangeably by z_c. With due regard to Kirchhoff's laws in Fig. 1(a), we arrive at the equivalent circuit in Fig. 1(b) where the compensator is represented as a passive RLC impedance, $i^\star$ translates to a current source, and the feedforward manipulates a controllable voltage source.

To illustrate how the compensator drives $i \to i^\star$, we consider a controller with proportional, integral, derivative, and resonant terms with the following transfer function

$$G_\mathrm{c}(s) = z_\mathrm{c}(s) = k_\mathrm{p} + k_\mathrm{i}\frac{1}{s} + k_\mathrm{d}s + \frac{k_\mathrm{r}s}{s^2 + \omega_\mathrm{r}^2}. \qquad (1)$$

This general controller is meant to highlight various applications where $i^\star$ could have dc as well as ac components. Simpler PI and PR implementations are straightforwardly recovered by discarding unneeded terms. Comparison of (1) to basic circuit laws allows us to obtain the passive RLC instantiation of z_c in Fig. 1(b) where the proportional, integral, derivative, and resonant terms correspond to a resistor, capacitor, inductor, and resonant tank which are cascaded to obtain the controller. In the circuit setting, PI and PR controllers are obtained by short-circuiting unused components.

Reflecting further on the equivalent circuit model, it is apparent that the error current, e, flows through z_c and the control effort, u, is the voltage across z_c. Here, ideal reference tracking at some frequency $\omega^\star$ is obtained when $\|z_\mathrm{c}(j\omega^\star)\| \to \infty$ such that z_c behaves as an open circuit and the only available path for the reference current is into the physical branch (i.e., $i \to i^\star$). This is obtained at dc for $\omega^\star = 0$ with a capacitive element, at some resonant frequency $\omega^\star = \omega_\mathrm{r}$ with an LC tank, at high frequencies $\omega^\star \to \infty$ with an inductor, and proportional control action maps straightforwardly as a resistor. With the circuit model, it is also clear that feedforward cancels voltage disturbances on the output of the converter.

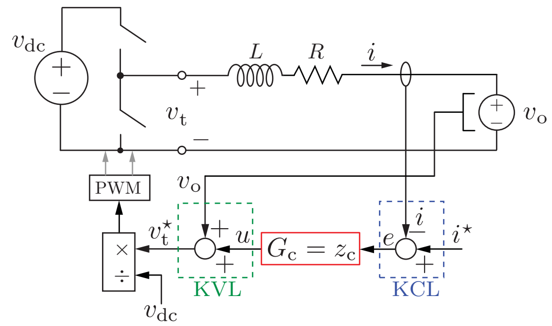

(a) half-bridge with current control

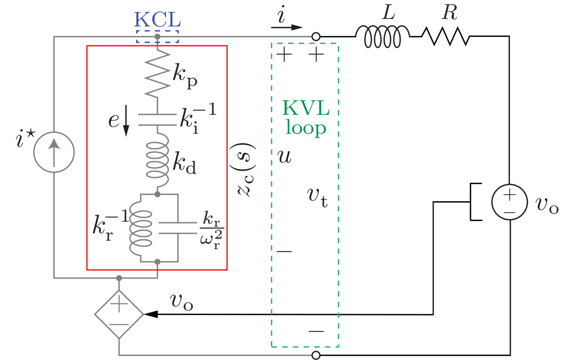

(b) equivalent circuit with generic PIDR compensator

Figure 1: A half-bridge converter with current control is depicted in (a). Kirchhoff's current and voltage laws are embedded within the input and output sides of the compensator and allow us to obtain the equivalent closed-loop circuit model in (b).

In the remainder of the paper, we apply the fundamental concepts illustrated in Fig. 1 to three-phase inverters. All analysis will be carried out in two-dimensional reference frames where dq and $\alpha\beta$ pertain to the synchronous and stationary reference frames, respectively. We adopt the short hand notation x^dq and $x^{\alpha\beta}$ to denote the following complex quantities:

$$x^\mathrm{dq} = x^\mathrm{d} + \mathrm{j}x^\mathrm{q}, \quad x^{\alpha\beta} = x^\alpha + \mathrm{j}x^\beta. \qquad (2)$$

Our study is restricted to balanced ac systems where the zero-axis component is discarded. Phase-locked-loop (PLL) and dc-side dynamics are also neglected and reserved for future work.

III. Circuit-Equivalent Models for Three-phase Inverters

We now apply the basic concepts sketched out in Section II to derive circuit-equivalent representations for inverters in the dq- and $\alpha\beta$-reference frames.

A. The Synchronous dq Reference Frame

We begin with the well-established model in Fig. 2(a) which depicts the cross-coupling between axes, the d- and q-axis control loops with PI compensators, and feedforward signals. Application of the concepts in Section II allow us to translate

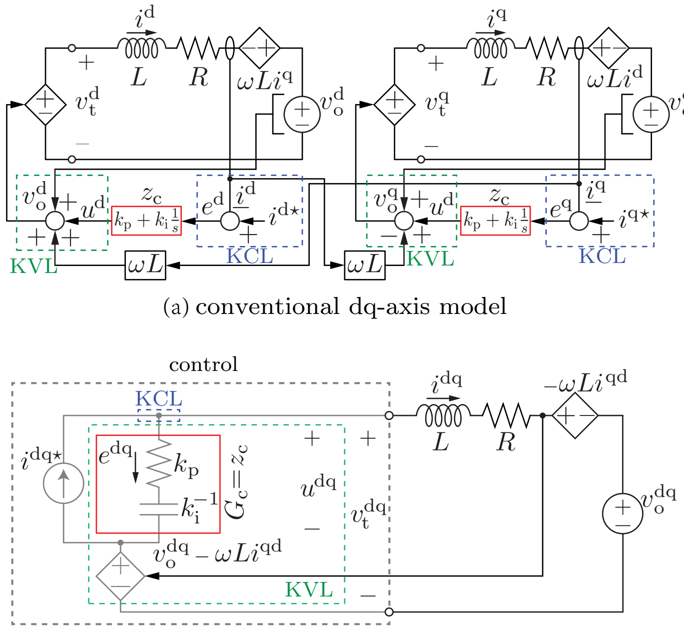

(a) conventional dq-axis model

(b) dq-axis circuit equivalent

Figure 2: (a) The conventionally drawn representation of a dq-axis model for a three-phase inverter with current control. (b) Equivalent circuit model where the feedback and feedforward paths are captured with circuit elements. Similar to the definition in (2), $x^{\rm qd} := x^{\rm q} - {\rm j}x^{\rm d}$.

this into the circuit representation in Fig. 2(b) where the PI compensator is an RC circuit, feedforward signals manipulate a voltage source, and the references are current sources. For convenience, we represent both axes compactly in a single circuit which admits complex-valued signals.

Unlike conventional transfer-function-based analysis where derivation of the closed-loop response requires several algebraic steps, the equivalent circuit gives this directly via the current divider rule. Assuming ideal sensing and feedforward cancellation of the $v_{\rm o}^{\rm dq} \pm \omega L i^{\rm qd}$ disturbance, the closed-loop response is

$$\begin{aligned} H(s) = \frac{i^{\rm dq}(s)}{i^{\rm dq\star}(s)} &= \frac{z_{\rm c}(s)}{z_{\rm c}(s) + z_{\rm f}(s)} \\ &= \frac{k_{\rm p} + k_{\rm i}/s}{(k_{\rm p} + k_{\rm i}/s) + (R + sL)}. \end{aligned} \tag{3}$$

The above formulation matches what is well-known in the literature [1]. The key difference being that we arrive at it via the application of a well-known circuit law and obtained it directly by inspection of a circuit. Now consider the control-synthesis problem where a typical objective is to determine the PI control gains, $k_{\rm p}$ and $k_{\rm i}$, such that $H(s)$ is a first-order system with time constant τ. To this end, we highlight the following result.

Theorem. The closed-loop transfer function, $H(s)$, is first-order with time constant, τ,

$$H(s) = \frac{1}{1 + \tau s}, \tag{4}$$

if and only if the time constant $\tau_{\rm c}$ of the RC circuit-equivalent of the PI compensator,

$$\tau_{\rm c} = \frac{k_{\rm p}}{k_{\rm i}}, \tag{5}$$

matches the time constant $\tau_{\rm f}$ of the inductive output filter:

$$\tau_{\rm f} = \frac{L}{R}. \tag{6}$$

Proof. To prove the forward direction, we begin by expressing

$$H(s) = \frac{k_{\rm p} s + k_{\rm i}}{Ls^2 + (R + k_{\rm p})s + k_{\rm i}} =: \frac{N(s)}{D(s)}. \tag{7}$$

For $H(s)$ (as expressed above) to match the desired first-order system representation in (4) with time constant τ, we need

$$D(s) = N(s)(1 + \tau s). \tag{8}$$

Matching coefficients, we can conclude that this implies $k_{\rm p} = L/\tau$ and $k_{\rm i} = R/\tau$, or equivalently, that $\tau_{\rm c} = \tau_{\rm f}$. To prove the reverse direction, with elementary algebraic operations, we can express

$$H(s) = \left(1 + \frac{1 + \tau_{\rm f} s}{1 + \tau_{\rm c} s} \cdot \frac{R}{k_{\rm i}} s\right)^{-1}. \tag{9}$$

From above, we can infer that if $\tau_{\rm c} = \tau_{\rm f}$, then $H(s)$ is a first-order transfer function with time constant $\tau = R/k_{\rm i}$. ■

A physical interpretation of the result above naturally emerges from the circuit-based model. In summary, it is a matching of the time-constants between each set of pairwise RC and RL circuit elements which gives a first-order circuit response. This interpretation is indeed qualitatively different from the frequency-domain notion of pole-zero cancellation in the closed-loop transfer function.

B. The Stationary $\alpha\beta$ Reference Frame

The classical current-controlled inverter model in the $\alpha\beta$ reference frame is illustrated in Fig. 3(a). Again, we apply the basic principles in Section II to arrive at the equivalent circuit model in Fig. 3(b). Since the reference signal and load voltage are sinusoidal, we adopt the typical strategy where the compensator takes on a PR form given by

$$G_{\rm c}(s) = z_{\rm c}(s) = k_{\rm p} + \frac{k_{\rm r} s}{s^2 + \omega_{\rm r}^2}, \tag{10}$$

where the compensator resonant frequency, denoted as $\omega_{\rm r}$, is chosen to coincide with the load (or grid) frequency (e.g., 50 or 60 Hz). Again, the resonant structure revealed in Fig. 3(b) clearly shows that $z_{\rm c}$ acts as a high impedance path at the resonant frequency.

Mirroring (3), the relationship between the current reference, $i^{\alpha\beta\star}$, and output current, $i^{\alpha\beta}$, is captured by the transfer function:

$$\begin{aligned} H(s) = \frac{i^{\alpha\beta}(s)}{i^{\alpha\beta\star}(s)} &= \frac{z_{\rm c}(s)}{z_{\rm c}(s) + z_{\rm f}(s)} \\ &= \frac{k_{\rm p}(s^2 + \omega_r^2) + k_{\rm r} s}{(s^2 + \omega_{\rm r}^2)(sL + R) + k_p(s^2 + \omega_{\rm r}^2) + k_{\rm r} s}. \end{aligned} \tag{11}$$

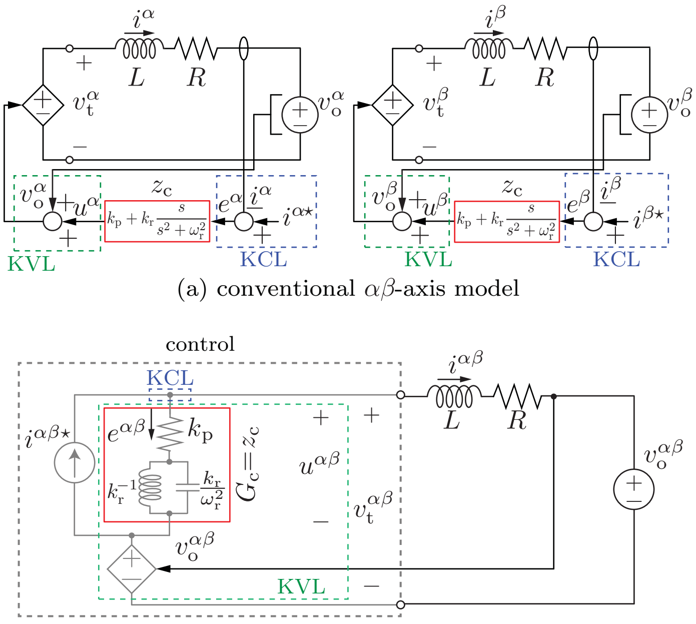

(a) conventional $\alpha\beta$-axis model

(b) $\alpha\beta$-axis circuit equivalent

Figure 3: (a) Equivalent $\alpha\beta$-axis model for three-phase voltage-source inverter with inductive output filter and current control. (b) Circuit representation capturing compensator action recovered leveraging KVL and KCL.

Note that $H(s)$ is third-order and is generally difficult to analyze. However, the circuit-equivalent provides insights that are leveraged to facilitate design. The PR compensator admittance $y_{\mathrm{c}} := z_{\mathrm{c}}^{-1}$ is given by:

$$y_{\mathrm{c}} = \frac{1}{z_{\mathrm{c}}} = \frac{1}{k_{\mathrm{p}}} \frac{s^2 + \omega_{\mathrm{r}}^2}{s^2 + \frac{k_{\mathrm{r}}}{k_{\mathrm{p}}} s + \omega_{\mathrm{r}}^2}. \tag{12}$$

Note that y_{c} has the same form as a notch filter (i.e., band-stop filter) [14] with center frequency ω_{r}. Furthermore, the ratio $k_{\mathrm{r}}/k_{\mathrm{p}}$ is related to the notch filter damping factor, ζ, and resonant frequency, ω_{r}, as follows:

$$\frac{k_{\mathrm{r}}}{k_{\mathrm{p}}} = 2\zeta\omega_{\mathrm{r}} = \frac{2}{\tau_{\mathrm{c}}}, \tag{13}$$

where τ_{c} is the time-constant of the compensator RLC branch. This is consistent with classical dynamical systems analysis where second order linear systems are known to have a time constant equal to $\zeta\omega_{\mathrm{r}}$. Rearranging terms in (11) allows us to isolate the dynamics of a notch filter, and yields

$$H(s) = \frac{k_{\mathrm{p}}}{\underbrace{\left(\frac{s^2 + \omega_{\mathrm{r}}^2}{s^2 + \frac{k_{\mathrm{r}}}{k_{\mathrm{p}}} s + \omega_{\mathrm{r}}^2}\right)}_{\text{notch filter}} (sL + R) + k_{\mathrm{p}}}. \tag{14}$$

Now we proceed to the design task and first select the proportional gain, k_{p}. Since the notch factor in (14) is in-effect inactive at frequencies sufficiently far from ω_{r}, the closed-loop response can be approximated as

$$H(s) \approx \frac{k_{\mathrm{p}}}{sL + R + k_{\mathrm{p}}} = \frac{k_{\mathrm{p}}}{k_{\mathrm{p}} + R}\left(1 + \frac{L}{k_{\mathrm{p}} + R} s\right)^{-1}, \tag{15}$$

at those frequencies. With the approximate first-order behavior in (15), we can engineer the response to have a user-defined cut-off frequency, denoted as ω_{c}, by choosing

$$k_{\mathrm{p}} = \omega_{\mathrm{c}} L - R, \tag{16}$$

where ω_{c} is sufficiently higher than ω_{r}. Here the circuit interpretation reveals that the compensator resistance, k_{p}, is equal to the difference between the physical-branch inductive reactance and resistance at ω_{c}.

We now shift focus to the resonant gain k_{r}. Mimicking the strategy used in the dq-domain above, we match the time constant of the second order compensator (as defined in (13)) with the time-constant of the phyical RL branch. This gives

$$\tau_{\mathrm{c}} = \frac{2k_{\mathrm{p}}}{k_{\mathrm{r}}} = \frac{L}{R}. \tag{17}$$

Substituting (16) into (17) yields the resonant gain

$$k_{\mathrm{r}} = 2\frac{R}{L} k_{\mathrm{p}} = 2\omega_{\mathrm{c}} R - 2\frac{R^2}{L}. \tag{18}$$

This completes the design procedure for the PR controller. Here we note that the circuit-based interpretation again shows that time-constant matching between cyber and physical circuit elements gives a systematic design approach.

IV. Simulation Results

To substantiate the performance of the above-mentioned PI and PR compensators with control gains obtained based on the

TABLE I
INVERTER FILTER AND CONTROLLER PARAMETERS.

Symbol	Details		
	Description	Value	Units
L	Filter inductance	1.5	mH
R	Filter resistance	0.5	Ω
ω_{r}	Resonant & grid frequency	$2\pi 60$	rad/s
ω_{c}	Cut-off frequency	$2\pi 300$	rad/s
k_{p}	Proportional gain of PI	2.83	Ω
k_{i}	Integral gain of PI	942	F^{-1}
k_{p}	Proportional gain of PR	2.33	Ω
k_{r}	Resonant gain of PR	1552	H^{-1}

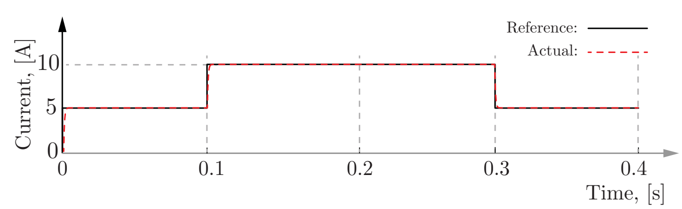

Figure 4: Performance of PI current controller in the synchronous dq reference frame.

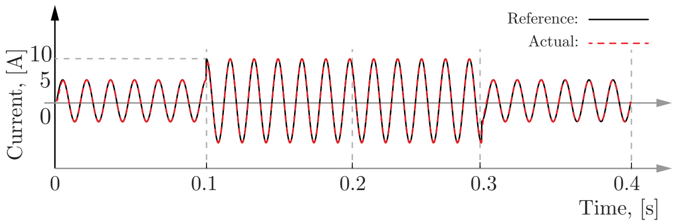

Figure 5: Sinusoidal waveforms associated with the inverter in the stationary $\alpha\beta$ reference frame.

circuit-equivalent model, two sets of simulations configured with system parameters listed in Table I were carried out. Figures 4 and 5 present the time-domain simulation results for the PI compensator and PR compensator, respectively. Due to the symmetry of the two-dimensional components, we only show the d-axis component i^{d} in the dq reference-frame and the α-axis component i^{α} in the $\alpha\beta$ reference-frame.

In Fig. 4, we can observe that the dc current tracking performance ($i^{\mathrm{d}} \rightarrow i^{\mathrm{d}\star}$) follows a first-order system response as required. In Fig. 5, we can also see that the current i^{α} tracks the current reference $i^{\alpha\star}$. This is accomplished with zero steady-state amplitude and instantaneous phase-tracking error and desired transient dynamics are achieved.

V. Conclusions & Future Work

In this paper, we derived unified circuit-equivalent representations capturing controller *and* filter dynamics for current-controlled inverters. Results were given in both the synchronous dq and stationary $\alpha\beta$ reference frames. A variety of circuit-theoretic notions and rules of thumb were then leveraged for controller design. As part of future work, we will aim to incorporate the PLL and dc-link dynamics into the circuit-based representation.

References

[1] A. Yazdani and R. Iravani, *Voltage-Sourced Converters in Power Systems*. Hoboken, NJ: John Wiley & Sons, Inc., 2010.

[2] J. Sun, "Impedance-based stability criterion for grid-connected inverters," *IEEE Transactions on Power Electronics*, vol. 26, pp. 3075–3078, Nov. 2011.

[3] L. Harnefors, M. Bongiorno, and S. Lundberg, "Input-admittance calculation and shaping for controlled voltage-source converters," *IEEE Transactions on Industrial Electronics*, vol. 54, pp. 3323–3334, Dec. 2007.

[4] J. Sun, "Small-signal methods for AC distributed power systems - A review," *IEEE Transactions on Power Electronics*, vol. 24, pp. 2545–2554, Nov. 2009.

[5] X. Wang, L. Harnefors, and F. Blaabjerg, "Unified impedance model of grid-connected voltage-source converters," *IEEE Transactions on Power Electronics*, vol. 33, pp. 1775–1787, Feb. 2018.

[6] L. Li, T. Jin, and K. M. Smedley, "A New Analog Controller for Three-Phase Voltage Generation Inverter," *IEEE Transactions on Industrial Electronics*, vol. 55, pp. 2894–2902, Aug. 2008.

[7] B. B. Johnson, S. V. Dhople, A. O. Hamadeh, and P. T. Krein, "Synchronization of Parallel Single-Phase Inverters With Virtual Oscillator Control," *IEEE Transactions on Power Electronics*, vol. 29, pp. 6124–6138, Nov. 2014.

[8] Q. Zhong and G. Weiss, "Synchronverters: Inverters that mimic synchronous generators," *IEEE Transactions on Industrial Electronics*, vol. 58, pp. 1259–1267, Apr. 2011.

[9] D. G. Holmes, T. A. Lipo, B. P. McGrath, and W. Y. Kong, "Optimized design of stationary frame three phase AC Current regulators," *IEEE Transactions on Power Electronics*, vol. 24, pp. 2417–2426, Nov. 2009.

[10] M. Yazdanian and A. Mehrizi-Sani, "Internal Model-Based Current Control of the RL Filter-Based Voltage-Sourced Converter," *IEEE Transactions on Energy Conversion*, vol. 29, pp. 873–881, Dec. 2014.

[11] R. Teodorescu, F. Blaabjerg, M. Liserre, and P. Loh, "Proportional-resonant controllers and filters for grid-connected voltage-source converters," *IEE Proceedings - Electric Power Applications*, vol. 153, p. 750, Sep. 2006.

[12] A. Kuperman, "Proportional-Resonant Current Controllers Design Based on Desired Transient Performance," *IEEE Transactions on Power Electronics*, vol. 30, pp. 5341–5345, Oct. 2015.

[13] D. N. Zmood and D. G. Holmes, "Stationary frame current regulation of PWM inverters with zero steady-state error," *IEEE Transactions on Power Electronics*, vol. 18, pp. 814–822, May 2003.

[14] B. Widrow, J. R. Glover, J. M. McCool, J. Kaunitz, C. S. Williams, R. H. Hearn, J. R. Zeidler, J. Eugene Dong, and R. C. Goodlin, "Adaptive noise cancelling: Principles and applications," *Proceedings of the IEEE*, vol. 63, pp. 1692–1716, Dec. 1975.